Final Report - CAM Lab

Team Members:

Cristiano Sartini
Simone Tumminello
Pietro Ughini

January 10, 2025

Contents

1 Notation and Formula

This section contains the notation and formulas used in the report.

1.1 Notations

Table 1: Notation for Milling

Symbol	Designation/Definition	Unit
a_e (face)	Radial depth of cut - width	mm
a_p (face)	Axial depth of cut - thickness	mm
a_e (peripheral)	Radial depth of cut - thickness	mm
a_p (peripheral)	Axial depth of cut - width	mm
DC	Cutting Diameter	mm
f_z	Feed per tooth	mm/tooth
z	Number of working teeth	pcs
Z	Number of teeth of the mill	pcs
φ	Total angle of contact	degree
φ_0	Angle of each tooth	degree
θ	Angle of working engagement	degree
k_r	Primary entering angle	degree
k_r'	Secondary entering angle	degree
λ_s	Back rake angle	degree
γ_0	Rake Angle	degree
h_D	Chip thickness	mm
h_D, av	Average chip thickness	mm
k_{cs}	Specific cutting pressure	N/mm^2
k_c	Cutting pressure	N/mm^2
n	Rotational speed of the mill	rpm
v_c	Cutting speed	mm/min
v_f	Feed velocity	mm/min
A_D	Chip section	mm^2
P_c	Cutting power	kW
T_c	Cutting Torque	Nm
F_c	Cutting force	N
r	Cutting radius	mm
R_a	Roughness	μm
t_c	Cutting time	second

Table 2: Notation for Drilling

Symbol	**Designation/Definition**	**Unit**
H	Cutting depth	mm
D	Drill diameter	mm
DCON	Connection diameter	mm
f_z	Feed per tooth	mm/rev
Z	Number of cutting edges	pcs
θ	Point angle	degree
h_D	Chip thickness	mm
k_c	Cutting pressure	N/mm^2
n	Rotational speed of the drill	rpm
v_c	Cutting speed	m/min
v_f	Penetration rate	mm/min
A_D	Chip section	mm^2
P_c	Cutting power	kW
M_c	Cutting Torque	Nm
F_c	Cutting force	N
MRR	Material Removal Rate	mm^3/min
t_C	Cutting time	second
t_M	Machining time	second

1.2 Formulas

Table 3: Formulas for Milling

Formula	**Description**	**Unit**
$v_f = Zf_zn$	Feed Velocity	mm/min
$n = \frac{v_c \cdot 1000}{\pi \cdot DC}$	Spindle speed	rpm
$\varphi_0 = \frac{2\pi}{Z}$	Angular distance between teeth	rad
$z = \frac{\varphi}{\varphi_0}$	Number of working teeth	pcs
$h_d = f_z \sin\theta$	Chip thickness (slab)	mm
$h_d = f_z \cos\theta \sin k_r$	Chip thickness (face)	mm
$h_m = \frac{f_z}{\varphi} \cdot \frac{2a_e}{DC}$	Average chip thickness	mm
$k_c = \frac{k_{cs}}{h_d^x}\left(1 - \frac{\gamma_0}{100}\right)$	Cutting pressure	N/mm^2
$A_d = h_d a_p$	Chip area	mm^2
$F_c = k_c A_d$	Cutting force	N
$T_c = \sum_{i=1}^{z} \frac{F_c \cdot DC}{2 \cdot 1000}$	Cutting torque	Nm
$P_c = T_c \frac{2\pi n}{60}$	Cutting power	W

Table 4: Formulas for Drilling

Formula	**Description**	**Unit**
$v_f = Z f_z n$	Penetration rate	mm/min
$n = \frac{v_c \cdot 1000}{\pi \cdot DC}$	Spindle speed	rpm
$h_d = \frac{f_z}{2} \sin\left(\frac{SIG}{2}\right)$	Chip thickness	mm
$k_c = \frac{k_{cs}}{h_d}$	Cutting pressure	N/mm^2
$A_d = \frac{f_z}{4} \cdot DC$	Chip area	mm^2
$F_c = k_c A_d$	Cutting force	N
$T_c = \frac{F_c \cdot DC}{2}$	Cutting torque	Nm
$P_c = T_c \frac{2\pi n}{60}$	Cutting power	W
$A_d = \frac{f_z}{4} \cdot (DC_{\text{ext}} - DC_{\text{int}})$	Chip area (reaming)	mm^2
$T_c = Z \frac{F_c \cdot (DC_{\text{ext}} - DC_{\text{int}})}{4}$	Cutting torque (reaming)	Nm

Table 5: Formulas for Roughness

Formula	**Description**	**Unit**
$R_a = \frac{f_z^2 \cdot 1000}{32 \cdot R}$	Roughness (slab)	μm
$R_a = \frac{f_z^2 \cdot 1000}{32 \cdot r}$	Roughness (where r is the nose radius, face milling)	μm
$R_a = \frac{f_z}{4 \cdot (\cot k_r' + \cot k_r)} \cdot 10^3$	Roughness (face milling)	μm

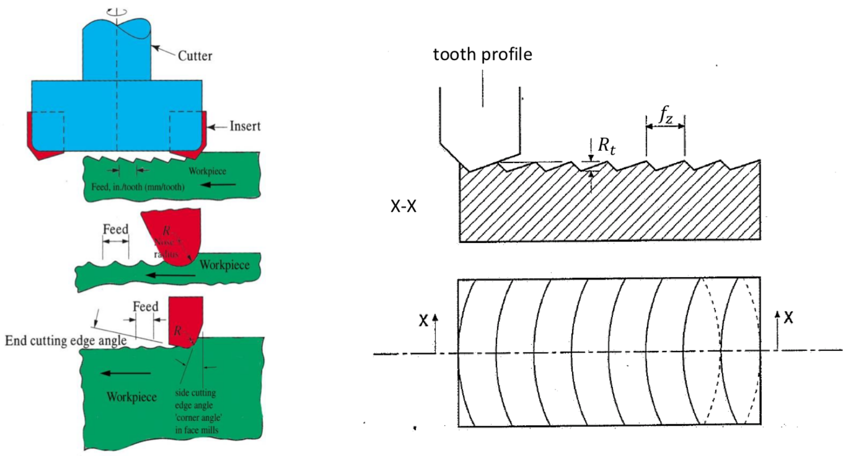

Roughness in Face Milling

2 Introduction of Project Product

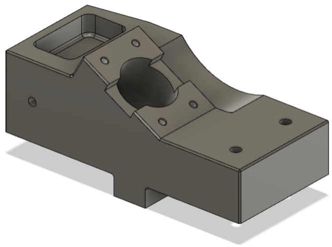

2.1 Inputs and Variables

Inputs

The aim of this project is to design a manufacturing process of a workpiece, which was given us through its 2D technical drawings. Starting from the realization in Fusion CAM software of the 3D and stock models, we managed to design a proper cutting routine to satisfy geometrical requirements expressed in 2D drawings (geometric tolerances and target roughness) and the machine parameters specified in the table below.

Information of the machine tool	
Working Area (mm)	1160 x 1000 x 900
Rapid Speed (m/min)	42
Maximum Spindle Rotational Speed (rpm)	14000
Spindle Power (kW)	16
Spindle Repositioning Time (s)	5
Tool Changing Time (s)	15
Loading and Unloading Time (s)	60

- The machine tool is a four-axis machine, and its initial spindle state is in the z direction. For a given setup, you can only choose one additional spindle direction for machining, either ±x or ±y.

- The fixture selection is limited to the one shown in the figure below; it can be scaled and modified on this model, but the clamping method for the part cannot be changed.

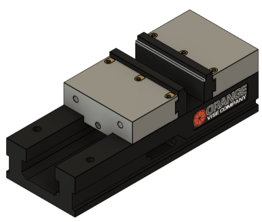

Variables

The part has a parametric design based on 4 parametric variables:

- **V1.** Workpiece material (4);
- **V2.** Threaded holes (3);
- **V3.** Tilted angle (3);
- **V4.** Stock size XYZ (3);

Variable	Description
V1	P1.3.Z.AN
V2	M7x1.0
V3	30 °
V4	264x126x128 mm

Workpiece Material - P.1.3.Z.AN -

Unlike the last three parametric variables, which talk about geometry requirements, **V1** is referred to the classification of the workpiece material, since it represents the material **MC code**. In metal cutting industry each material, with its own properties (e.g. presence of alloying elements, heat treatment, hardness, surface skin, etc.), influences the workpiece's machinability, namely the ability of the workpiece to be machined by ensuring an undisturbed cutting action, a fair tool life and a suitable chip formation. Together with machinability, materials properties influence cutting tool geometry, grade and cutting data. To make this choice easier ISO has created a standard of 6 majors groups, each one with unique machinability properties. In order to go give even more specific recommendations to assist in improving productivity, Sandvik Coromant has generated MC code as a new material classification with a more detailed structure composed by numbers and letters that identify even more subgrops.

Regarding our workpiece's material:

- **P**: Steel material group in according with ISO standard, an iron based alloy classified by its carbon content; ranging from unalloyed to high-alloyed material and including steel casting and ferritic and martensitic stainless steels.
- **P.1**: unalloyed steels subgroup, which share a carbon content lower than 0.8%, composed solely of iron (Fe), with no other alloying elements.
- **P.1.3**: unalloyed steels with a high carbon content ($C \geq 0.55\%$). A higher carbon content enables hardening of the material and so increasing abrasive wear, fragility and thermal handling. Low carbon steels ($C \leq 0.2\%$) indeed are more ductile, therefor leading to adhesive wear and so built-up edge (bue); but also to an higher plastic deformation tendency, which can help in obtaining a continuous and longer chip, rather than the discontinuous one of brittle materials.
- **P.1.3.Z**: Z is the manufacturing process: forged/rolled/cold down. Rolled steel exhibits a large grain size, causing variations in cutting forces, while forged steel has a more uniform structure due to its smaller grain size.
- **P.1.3.Z.AN**: AN stands for Annealing as heat treatment, it decreases the hardness to increasing ductility, and it also removes internal tensions originated in forging and rolling.

Additional information have been given to us regarding material's machinability:

- Specific cutting force $k_{c1} = 1750$ N/mm^2: the force in cutting direction normalized by 1 mm^2 area, depending on the material group.
- A coefficient $m_c = 0.25$ to compute the actual specific cutting force k_c.

2.2 Features and Operations

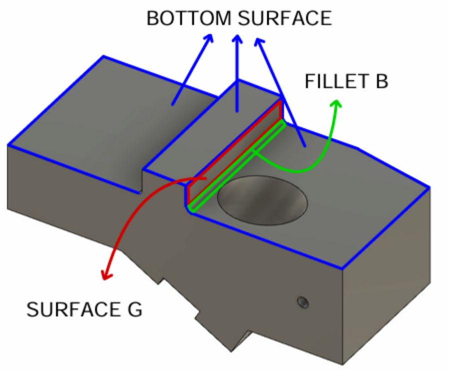

SETUP 1

Feature	Operation
Bottom Surface	**BS_F**: Face → Face Milling
	BS_P: Pocket → Flat End Milling
Surface G	**SG_C**: Contour → Flat End Milling
Fillet B	**FI_B**: Pencil → Ball End Milling
Surface D	**SD_F**: Face → Face Milling
Hole A	**HA_D**: Drilling
Chamfer	**CH_1**: Chamfer → Chamfer Milling
Surface C	**SCE_C**: Contour → Flat End Milling
Surface E	

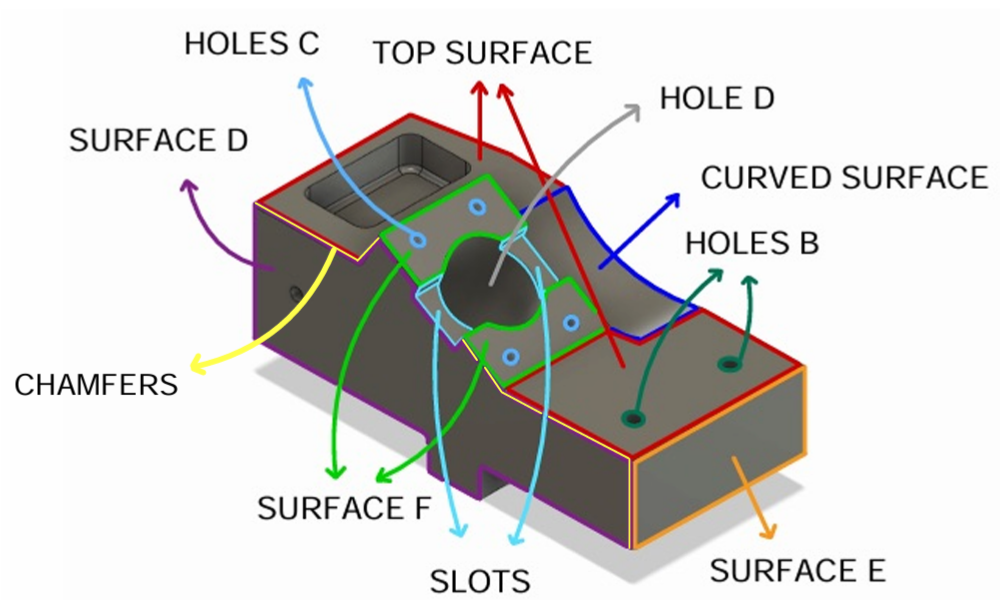

SETUP 2

Feature	Operation
Top Surface	**TS_F**: Face → Face Milling
	TS_P_U: Pocket → Flat End Milling
	TS_P_D: Pocket → Flat End Milling
Pocket	**PO_P**: Pocket → Flat End Milling
	PO_P_F: Pocket F. → Flat End Milling
	PO_FI: Pencil → Ball End Milling
Holes B	**HB_D**: Pilot Drill → Drilling
	HB_CB: Counterbore → Drilling
	HB_R: Reaming → Reaming
	HB_T: Thread → Thread Milling
Curved Surface	**CS_T**: Trace → flat End Milling
Fillet A	**FI_A**: Pencil → Ball End Milling
Surface F	**SF_P**: Pocket → Flat End Milling
	SF_P_F: P. Finishing → Flat End Milling
Surface H	**SH_P**: Pocket → Flat End Milling
Hole D	**HD_D**: Drilling
	HD_B: Boring
Slots	**SL_P**: Pocket → Flat End Milling
Holes C	**HC_D**: Pilot Drill → Drilling
	HC_CS: Countersink → Drilling
	HC_T: Thread → Thread Milling
Chamfer	**CH_2**: Chamfer → Chamfer Milling

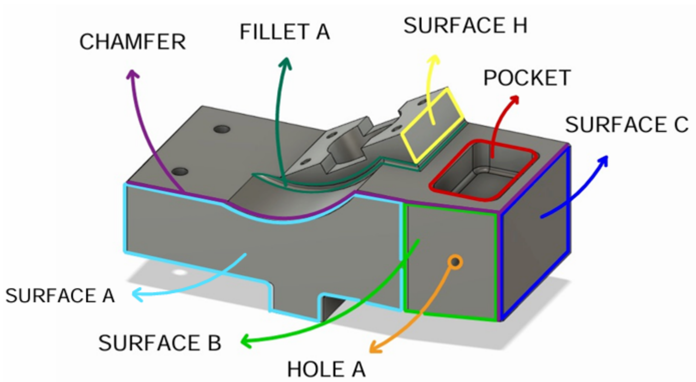

SETUP 3

Feature	Operation
Surface A	**SA_F**: Face → Face Milling
Surface B	**SB_F**: Face → Face Milling
Curved Surface	**CS_C**: Contouring → Flat End Milling
Chamfer	**CH_3**: Chamfer → Chamfer Milling

2.3 Precedence Graph

Process planning involves as a fundamental step the definition of sequences among operations, in order to create the features without violating the technical requirements. For this reason, it is useful to define a temporal hierarchy in machining operations, which can be done by reporting a precedence graph.

The graph has to be designed following these 2 **basic rules**:

- **Rule 1**: for each operation we perform first roughing and then finishing (trivial);
- **Rule 2**: we first machine a surface and then its hole(s) and pocket(s);

Among the various operations with high geometrical requirements, some of them are more critical, because achieving a high surface finishing or a specific geometry can be compromised by the order in which operations spatially close to them are performed. Therefor, it becomes necessary to define some special requirements in terms of **special rules** applied on the graph:

- **Special requirement 1**: we machine the large through hole before the slots, to ensure a better distribution of reactive forces on the milling cutter, otherwise we would have a discontinuity by machining from closely the tilted surface stock *(green part of the stock)* to the missing stock of the adjacent slot *(red part of the stock)*. In this why we are preventing sudden changes of load on cutting tool during the contouring finishing operation, that would have compromised the required roughness $R_a = 3.2$

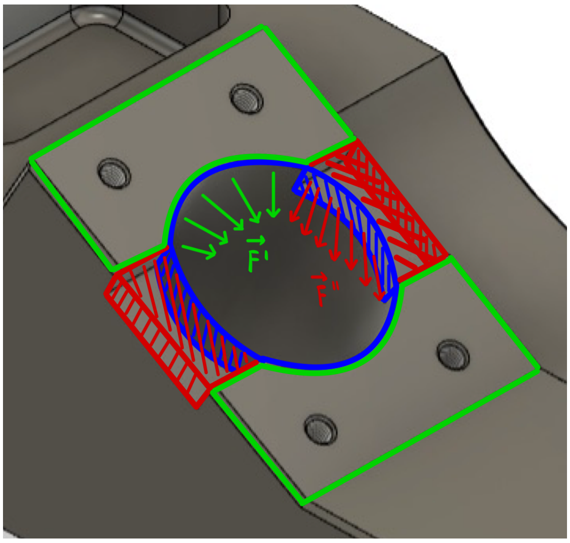

- **Special requirement 2**: throughout the pocket based on PO_P - PO_FI - PO_P_F operations, we impose pocket finishing operation before the pencil operation. This decision was made to avoid a too big a_e, since the tools designed for fillets are not made to plunge in the material and performe a slotting operation as explained in the catalog.
- **Special requirement 3**: after drilling the pilot holes B and C, we impose counterboring and countersinking operations before threading, to avoid causing the internal

thread to fall and thus forming, which could lead to a cross-tailed thread. In addition, we can enhance the concentricity between the counterbore/countersink and the pilot hole (and so of the following thread).

- **Special requirement 4**: Regarding the creation of chamfers through the three setups, since they are a feature involving two or more surfaces (connecting them via an inclined edge), we decided to first perform roughing and finishing operations of the adjacent surfaces performed in the same setup. This approach allows us to address the following issues:
  - Prevent the risk of subsequent milling operations on adjacent faces damaging the already created chamfers.
  - Ensure that the chamfers are based on the final geometry of the surfaces, as refining these surfaces afterward could compromise the quality and consistency of the chamfers.
  - Similarly to fillets, we do not want chamfer milling treated as if it were axial slot milling with an angled tip. Instead, we want the tool to work in an area free of stock, at least on one of the adjacent surfaces, which therefore must already be machined.

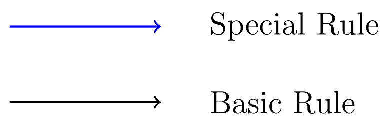

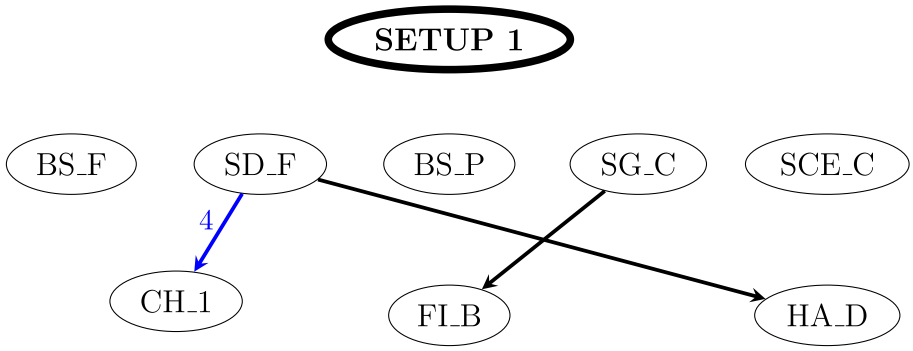

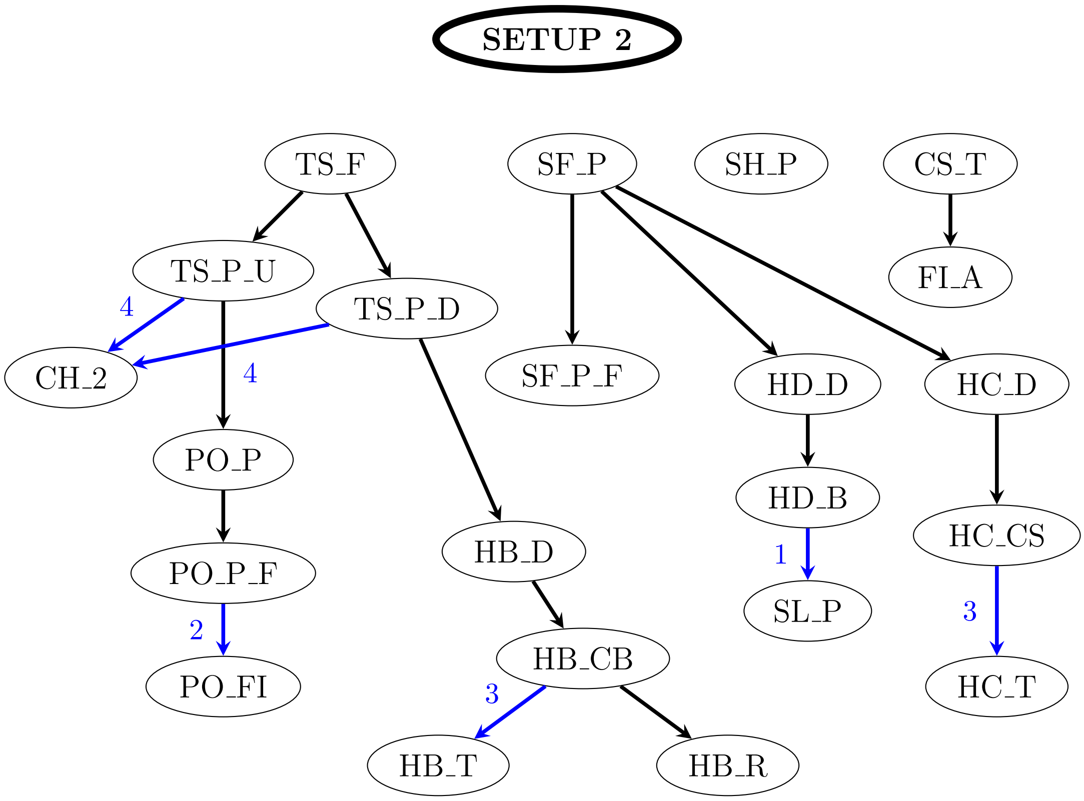

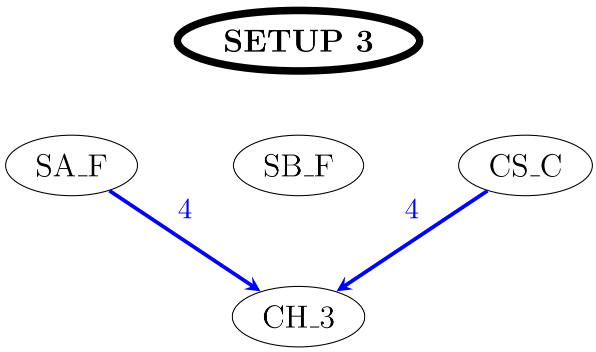

Remark: The division of the precedence graph into three setups is an intentional choice to make the representation clearer. Naturally, if we were to merge the three graphs into a single large graph, new precedence relationships would emerge between the operations of one setup and those of the next. In our representation, these relationships are implicitly conveyed through the separation into setups and the fact that the setups must be executed in the order in which they are numbered. This approach favors our representation by making it more concise and streamlined.

3 Detailed Final Solution to Realize Your Product

This section provides a detailed explanation of the final solution.

3.1 Throughput of the Product

For simplicity, in this paragraph, we will explain the product throughput in parts per hour and include the already sequenced operations in the table, instead of addressing them in Section 3.2.

Details	Machining Time [s]	Tool Changing Time [s]	Loading and Unloading Time [s]	Spindle Repositioning Time [s]
BS_F	104	0	30	0
SD_F	82	0	0	5
HA_D	8	15	0	0
CH_1	14	15	0	0
BS_P	232	15	0	5
SG_C	25	0	0	0
FI_B	27	15	0	0
SCE_C	128	15	0	0
TS_F	82	0	60	0
TS_P_D	204	15	0	0
TS_P_U	196	0	0	0
SF_P	173	0	0	5
SH_P	15	0	0	5
PO_P	136	15	0	5
CS_T	71	15	0	0
PO_P_F	53	15	0	0
SF_P_F	56	0	0	5
HD_D	19	15	0	0
HD_B	12	15	0	0
SL_P	59	15	0	0
HC_D	3	15	0	0
HC_CS	11	15	0	0
HC_T	27	15	0	0

Details	Machining Time $[s]$	Tool Changing Time $[s]$	Loading and Unloading Time $[s]$	Spindle Repositioning Time $[s]$
FI_A	23	15	0	5
PO_FI	23	0	0	0
HB_D	3	15	0	0
HB_CB	3	15	0	0
HB_R	1	15	0	0
HB_T	11	15	0	0
CH_2	57	15	0	0
SA_F	54	0	60	0
SB_F	30	0	0	5
CS_C	67	15	0	5
CH_3	7	15	30	0

ASSUMPTION: *Given that the loading and unloading time is 60 seconds, we assumed the following: at the beginning of the first setup, only loading the part is required (30 seconds); at the end of the final setup, only unloading the part is necessary (30 seconds); and between setups, both unloading and reloading the part are needed (60 seconds).*

Total time = 2586 seconds = 43 minutes and 6 seconds

$$\textbf{THROUGHPUT} \approx 1,4 \ \frac{\text{parts}}{\text{hour}}$$

3.2 Detailed Information for Your Setups

We have decided to develop the entire manufacturing process using three setups, each corresponding to a different way of positioning the part with respect to the fixture. Each setup is designed to satisfy the geometrical tolerance requirements while heuristically minimizing the total loading and unloading time.

In the following section, we briefly describe each setup, highlighting the specific geometrical tolerances it addresses and the tool accessibility challenges it seeks to overcome.

Before going into the details, we outline the two main reasons that led us to select three setups. First, it is important to note that minimizing the number of setups does not always result in the shortest machining time. For instance, reducing the number of setups might limit the ability to use the most time-efficient operation for a specific feature, ultimately increasing the overall machining time.

Here we present the two main reasons supporting the 3 setups choice:

- **Technical Infeasibility of Two Setups**:

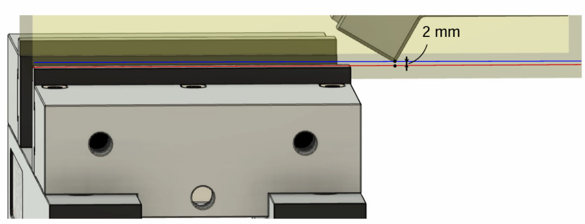

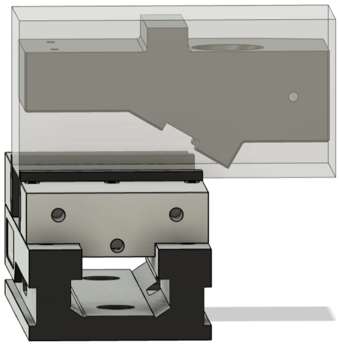

Given that *Surface D* is a datum (*datum B*), it must be entirely machined in a single pass. To respect this tolerance while minimizing the number of setups, we aimed to position the part in a way that allows the machining of both the *bottom surface* and all the *lateral surfaces* (including precisely *Surface D*) in a single setup. The final configuration (the only approach that we found which satisfied the above-mentioned condition) , shown in the right image above, involves clamping the lateral and bottom stock while leaving the most protruding part of *Surface D* outside the clamping area. This approach was intended to mitigate the potential accessibility issues caused by the proximity of the vise jaw. At this point, we decided to entirely machine *Surface D* using a 2D contouring operation, where a flat end mill removes material along the entire length, from the beginning of the stock to the line ideally passing through the end of the *Surface D* protrusion. However, this setup presents a critical issue that makes it unfeasible: by performing peripheral milling precisely up to the extremity line (*blue line in the left image above*), there is a risk of size errors when machining the edge between *Surface F* and *Surface H* in the subsequent operation; but at the same time, we can only exploit a 2 mm offset length up to the adjacent jaw's upper surface (*red line in the image*), which would introduces the risk of unwanted contact with the fixture.

- **Need for at least Two Setups**: Considering the geometrical tolerance requirements, which relate datum A (*bottom surface*) to the annotated features on the *tilted surface* and *top surface*, it is not feasible to respect these tolerance specifications if the part is clamped in contact with these features. In fact in that case we would be forced to machine some feature partially, due to the presence of the vise jaws.
  Therefore, throughout the setups, we have decided to have a clamping contact exclusively with the lateral surfaces A, B, C, D, and E.
  Based on this assumption, it has become clear that machining the *top surface*, *tilted surface*, and *bottom surface* requires at least one setup change. This is due to accessibility constraints of the cutting tool, which cannot come into contact with either the jaws or the central part of the vise body when the *bottom surface*, *tilted surface*, or *top surface* is positioned opposite to the functionally free surface.

SETUP 1

Positioning: The initial stock is clamped on the smallest lateral faces, allowing the lateral face which covers the *Surface D* to protrude. This configuration creates a tool-accessible area where the free portion of the stock is functional to the machining of the *Bottom surface* and the *Lateral surfaces*.

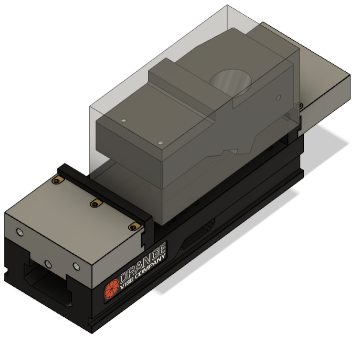

Satisfied Geometrical Tolerances

1. Realization of Surface D as **Datum B**.
2. **Surface Parallelism** between Surface G and its **Datum C**, that is Surface E.
3. Realization of Bottom Surface as **Datum A**.

SETUP 2

Positioning: The two jaws clamp the already machined shorter lateral surfaces (*Surface C* and *Surface E*), leaving the portion of the stock required for all features related to the *Top Surface* and *Tilted Surface* accessible. To ensure a uniform distribution of clamping forces, the part is symmetrically positioned by centering the jaws with respect to the midpoint of the fixed lateral surfaces.

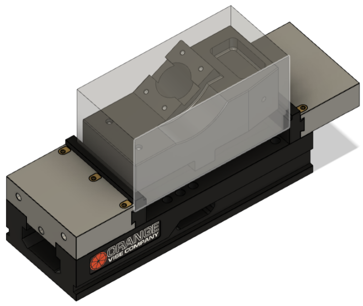

Satisfied Geometrical Tolerances

1. All the **Surface Parallelisms** related with **Datum A**, involving the Pocket and the Top Surface; by positioning the part as rotated of 180° around the axis parallel to the vise body, with respect the previous positioning.
2. Realization of the Tilted Surface as **Datum F**.
3. **Axis Perpendicularity** of Hole D with respect to **Datum D**, achieved by performing the roughing and finishing drilling operations for Hole D immediately after the finishing operation of the Tilted Surface. This approach preserves the spindle orientation between the machining of the two features, keeping constant also the positioning of the part.

4. Realization of Hole D as **Datum F**, achieved by completing its machining entirely within this setup, and by following Special Requirement 1.

5. **Axis Perpendicularity** of Holes C with respect to **Datum D** and **Datum F**, by performing Holes C, Hole D and Tilted Surface in this same setup, within the same constant spindle orientation.

SETUP 3

Positioning: The two jaws symmetrically clamp the previously machined shorter lateral surfaces (*Surface C* and *Surface E*) along their smaller side edges. This configuration facilitates the facing of the remaining *Surface A* and *Surface B*, as well as the contouring of the *Curved Surface* and the remaining chamfer.

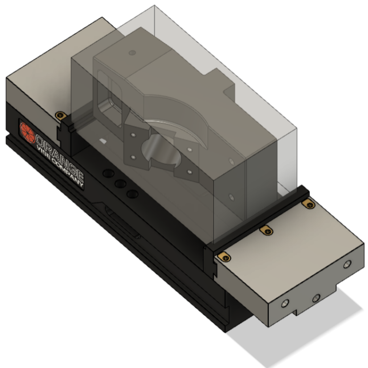

Process parameters are adressed in section 4.

3.3 Manufacturing Resources

The tool codes listed in the following tables are clickable links that redirect to the respective product pages on the Sandvik Coromant website. This allows for easy access to detailed specifications and additional information about the tools and inserts.

Face Milling Operations - Tool and Insert Codes with Links

Code_op.	**Tool Link**	**Insert Link**
BS_F	R245-100Q32-18M	R245-12T3M-PM 4330
SD_F	R245-100Q32-18M	R245-12T3M-PM 4330
TS_F	R245-100Q32-18M	R245-12T3M-PM 4330
SA_F	R245-080Q32-18M	R245-12T3M-PM 4330
SB_F	R245-080Q32-18M	R245-12T3M-PM 4330

Face with Flat end Mill - Tool Codes and Links

Code_op.	Tool Link
BS_P	1P222-2000-XA 1630
TS_P_D	1P240-2500-XA 1630
TS_P_U	1P240-2500-XA 1630
SF_P	1P240-2500-XA 1630
SH_P	1P240-2500-XA 1630
PO_P	1P222-1600-XA 1630
CS_T	1P260-0600-XA 1620
PO_P_F	1P222-1000-XA 1630
SF_P_F	1P222-1000-XA 1630
SL_P	1P222-1000-XA 1630

Chamfer and Fillet - Tool Codes and Links

Code_op.	Tool Link
FI_B	R216.42-06030-AI06G 1610
FI_A	R216.42-06030-AI06G 1610
PO_FI	R216.42-06030-AI06G 1610
CH_1	1C050-0150-045-XA 1620
CH_2	1C050-0150-045-XA 1620
CH_3	1C050-0150-045-XA 1620

Peripheral Operations - Tool Codes and Links

Code_op.	Tool Link
SG_C	1P222-2000-XA 1630
SCE_C	2P370-2000-PB 1740
CS_C	1P240-2500-XA 1630

Drilling operations - Tool Codes with Links

Code_op.	Tool Link	Central Insert Link	Peripheral Insert Link
HA_D	861.1-0800-120A1-GM		
HB_D	860.1-0675-055A1-PM		
HB_CB	MFE0980X02S100		
HC_D	860.1-0600-019A1-PM		
HC_CS	DLE1000S100P090		
HD_D	880-D5000L40-03	880-08 05 08H-C-GR	880-08 05 W12H-P-GR 4334

Threading operations - Tool Codes with Links

Code_op.	**Tool Link**
HB_T	R217.14C060125AK17N
HC_T	R217.14C045100AC13N

Reaming operations - Tool Codes with Links

Code_op.	**Tool Link**
HB_R	835.B-1000-A1-PF

Boring operation - Tool Code with Link

Code_op.	**Tool Link**	**Insert Link**
HD_B	825D-56TC09U-C4L	TCMT 09 02 04-PF 4415

4 Verification of Operations

In this section, we will first provide a general explanation of the approach we used to validate the feasibility of each operation. Then, we will present a table containing some of the data used for each operation, along with the corresponding power and spindle speed required for that particular case as proof.

The six main categories of operations we used to address all the tasks required for the creation of the workpiece were:

- **Face milling**
- **Peripheral milling**
- **Drilling**
- **Reaming**
- **Thread milling**
- **Boring**

Face Milling case study

We categorized the following under the face milling case study: all face operations (performed using face milling cutters with inserts), all pocket operations (performed using solid carbide end mills), and finally, the pencil and chamfer operations. Since dedicated formulas are not available for pencil and chamfer operations, they can be easily verified using the face milling formulas with appropriate parameter adjustments.

- **Face milling tools with inserts**: The first step for standard face milling operations is to select the appropriate tool. To do this, it is necessary to consider the surface dimensions, determine arbitrarily but thoughtfully the number of radial passes, and consequently define a_e (radial cutting depth). Based on a_e, and using the rule of thumb provided in the catalog handbook ($D_c = \frac{3}{2} \cdot a_e$), the cutting diameter of the tool can be selected. Initially, assuming the surface will be milled in a single axial pass, we choose a_p equal to the surface depth and then select a tool with the previously determined diameter and a sufficiently large maximum axial depth of cut: APMX (APMX $\geq a_p$).

  After selecting the tool based on diameter and APMX and after collecting all its characteristics (like the number of teeth (Z)), the insert is chosen according to the workpiece material. The catalog then provides recommended values for cutting velocity (v_c) and feed per tooth (f_z), along with their respective maximum and minimum limits, based on the insert material (e.g. GC4330). Since our material was not listed, we used linear interpolation to determine the appropriate values for our case.

  Now let's go into the details of the formulas used to calculate power and spindle rotational speed. For the spindle rotational speed (n), once the cutting velocity (v_c) and the tool diameter (D_C) were known, we directly computed it $n = \frac{1000 \cdot v_c}{DC \cdot \pi}$.The procedure to validate the feasibility of n is trivial and is valid for every kind of operation: we checked if the value was above the maximum spindle rotational speed and if so, we reduced v_c always remaining within its specified range.
  On the other hand,in order to calculate the feed velocity we exploited the feed per tooth (f_z) and the number of teeth (Z): $v_f = n \cdot f_z \cdot Z$.

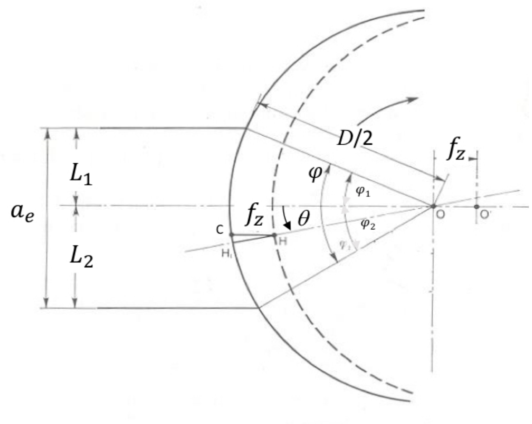

phi 1 and phi 2

Next, we decided to set $\varphi_2 = -90°$ for each operation (based on the tool's approach to the surface $\longrightarrow$ small engagement case always) and calculated φ_1 as follows:

$$\varphi_1 = \arcsin\left(\frac{a_e - DC/2}{DC/2}\right)$$

From φ_1, we calculated $\varphi = \varphi_1 + |\varphi_2|$, and using the number of teeth (Z) of the tool, we determined $\varphi_0 = \frac{360°}{Z}$. Using these values, we derived a crucial parameter:

the number of working teeth, $z = \frac{\varphi}{\varphi_0}$. This parameter allowed us to identify in which of the three power calculation cases we were:

- $z \leq 1$
  In the first case, calculating the maximum cutting power required is relatively straightforward, Since the worst-case scenario occurs near the maximum chip thickness, which corresponds to $\theta = 0$ (the angular position of the working tooth), the calculations focus on this critical point. In particular we need to compute the maximum chip area per tooth, given by: $A_{D,\max} = A_D(\theta = 0) = f_z \cdot a_p$
  The maximum cutting force is then calculated as: $F_{C,\max} = k_{C,\max} \cdot A_{D,\max}$
  where: $k_{C,\max} = k_{CS} \cdot \left(h_{D,\max}^{-x}\right) \cdot \left(1 - \frac{\gamma_0}{100}\right)$
  From these values, the cutting torque is determined using: $T_C = \frac{F_{C,\max} \cdot (D_C/2)}{1000}$
  Finally, the cutting power is calculated as:

  $$P_C = T_C \cdot \omega$$

  where the angular velocity (ω) is given by: $\omega = \frac{2\pi n}{60}$
- $1 < z \leq 2$
  In case number 2, the worst-case scenario occurs when the two cutting edges are cutting simultaneously:
  For tooth 1: $F_C(\theta_1) = k_{C,\theta_1} \cdot A_{D,\theta_1}$
  For tooth 2: $F_C(\theta_2) = k_{C,\theta_2} \cdot A_{D,\theta_2}$,
  where $\theta_2 = \theta_1 - \varphi_0$. Consequently, the cutting torque is calculated as:

  $$T_C = \frac{(F_C(\theta_1) + F_C(\theta_1 - \varphi_0)) \cdot (D_C/2)}{1000}$$

  To find the maximum torque and, by multiplying with ω, the maximum power, it is sufficient to derive this torque expression with respect to θ_1. This yields $\theta_{1,\max} = \varphi_0/2$ and consequently $\theta_{2,\max} = -\varphi_0/2$.
  It is crucial to ensure that these values can be used in the power calculation only when the conditions $\varphi_0/2 \leq \varphi_1$ and $-\varphi_0/2 \geq \varphi_2$ are satisfied. If these conditions are not met, it is appropriate to use $\theta_1 = \varphi_1$ and $\theta_2 = \theta_1 - \varphi_0$ instead, since for $\theta_{1,\max} = \varphi_0/2$ the first curring edge is not even in contact with the workpiece and therefore the result will not be the worst case.
- $z > 2$
  In this final case, the considerations are similar to the previous scenarios, but an additional assumption is made to estimate the maximum power: the use of the average chip thickness. It can be demonstrated that the cutting power is given by:

  $$P_C = \frac{k_{C,\text{av}} \cdot (a_e \cdot a_p \cdot v_f)}{60 \cdot 1000}$$

Once the maximum required cutting power P_c is determined, if this value is within the maximum power available, the operation is feasible. In this case, one can adjust the values of f_z (feed per tooth) and v_c (cutting speed), for example, increasing these values to optimize the operation time. If P_c exceeds the maximum power, however, it is still possible to adjust f_z and v_c by reducing their values within their respective ranges. Alternatively, if this adjustment is not sufficient, multiple passes can be performed, reducing a_p (depth of cut) and consequently the required power, until the operation becomes feasible again.

Table 6: Face Milling Operations

Code_op.	**ae**	**ap**	**Vc**	**fz**	**n [rpm]**	**Pc [W]**
BS_F	63	3.5	355	0.28	1130,000096	15718.1
SD_F	66	2.5	355	0.28	1130,000096	11626.2
TS_F	63	3.5	355	0.28	1130,000096	15718.1
SA_F	53	2.5	355	0.28	1412,50012	11657.1
SB_F	38	4.8	355	0.27	1412,50012	15674.9

- **face milling with flat end mills**: For surface machined with flat end mills, the procedure for selecting f_z and v_c differs slightly from the one used for traditional face mills with inserts, although the formulas for the three power calculation cases remain the same. Similar to the previous scenario, the tool selection is based on the size of the surface and the depth to be cut, ensuring the tool diameter is appropriate and that $APMX \geq$ cutting depth, just as before.

  The values of f_z and v_c are then chosen based on the recommended values of a_p and a_e from the catalog, depending on the type of operation (slotting, shoulder milling, pocket milling, etc.), and are determined by the workpiece material.

  Once these values are set, the required cutting power in the worst-case scenario can be calculated as previously illustrated. If the calculated power exceeds the maximum deliverable power, multiple passes can be performed by reducing a_p, ensuring the operation is feasible.

  Reducing a_p does not cause issues since the suggested values of f_z and v_c are provided assuming a_p is at its recommended level. If a_p decreases, the values for f_z and v_c remain valid. Problems arise only if a_p exceeds the recommended value, as this could damage the tool.

Table 7: Face with Flat end Mill

Code_op.	**ae**	**ap**	**Vc**	**fz**	**n [rpm]**	**Pc [W]**
BS_P	10	20	175	0.09	2785,211504	15851.4
TS_P_D	12.5	16	175	0.115	2228,169203	15240.5
TS_P_U	12.5	11	175	0.115	2228,169203	10477.9
SF_P	12.5	13.85640646	175	0.115	2228,169203	13198.7
SH_P	12.5	11	175	0.115	2228,169203	10477.9
PO_P	16	8.5	145	0.08	2884,683344	7880.7
CS_T	6	3	145	0.03	7692,488916	940.8
PO_P_F	10	3	145	0.05	4615,49335	1955.1
SF_P_F	10	5	145	0.05	4615,49335	3258.6
SL_P	10	5	145	0.05	4615,49335	3258.6

- **pencil and chamfer**: Regarding pencil and chamfer operations, the same considerations made earlier apply (since no specific formulas were provided in the handbook for this type of operation and power requirements were usually very low, we approximated them using face milling formulas). The main difference lies in the fact that, in Fusion360, pencil and chamfer operations do not allow for multiple passes, despite the fact that the recommended values for a_e and a_p from the catalog are quite low, which would typically not allow for a single pass.

  To overcome this issue and remain consistent with the software used, we decided to take the recommended values of f_z (feed per tooth) and v_c (cutting speed) from the catalog and apply a rule of thumb to account for tool wear, for example, by halving them. In some cases, halving v_c was not sufficient to meet the spindle rotational speed requirement, and therefore, further reduction of v_c was necessary.

Table 8: Chamfer and Fillet

Code_op.	ae	ap	Vc	fz	n [rpm]	Pc [W]
FI_B	3	3	150	0.04	7957,747155	1156.3
FI_A	3	3	150	0.04	7957,747155	1156.3
PO_FI	3	3	150	0.04	7957,747155	1156.3
CH_1	3	1.5	100	0.02	10610,32954	497.5
CH_2	1.5	1.5	130	0.02	13793,4284	482.3
CH_3	1.5	1.5	130	0.02	13793,4284	482.3

Peripheral Milling case study

Regarding peripheral milling, we focused on the subcategory of slab milling, as it coherently represents contour operations. This type of operation, along with trace, were the only ones we had to treat as slab milling to perform the power calculation.

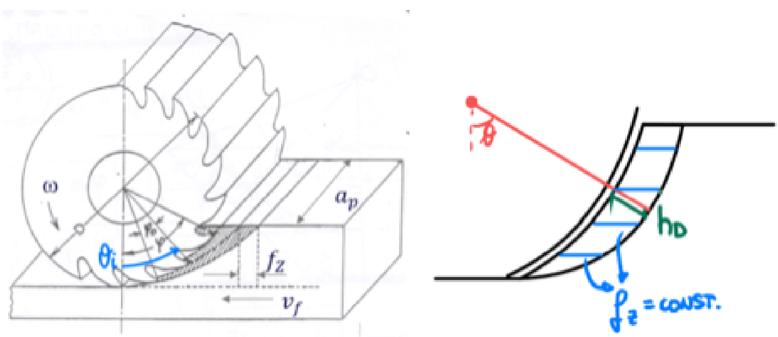

Figure 1: Peripheral Milling

The procedure for selecting the tool and the parameters necessary for the power calculation (a_e, a_p, v_c, f_z) within the catalog was the same as in the case of face milling with a flat end mill. However, particular attention was given, in the case of high-feed side milling, to the reduced dimension of a_e, which was often $0.25 \cdot DC$.
Once again, it was necessary to divide the power cases based on the number of working

teeth (z). Since we have already illustrated the formulas used in different scenarios for face milling, we will not repeat all the steps, as there are many similarities.
In fact, while the formulas largely remain the same, the main difference lies in calculating the maximum chip thickness required for determining the maximum power. In this case, as described in Section 1:

$$h_{D,\max} = h_D(\theta = \varphi) = f_z \cdot \sin(\varphi)$$

As a result of this formula, the maximum chip area and the maximum cutting pressure also change, as they depend on the chip thickness.

To satisfy the maximum power limits, we again relied on multiple passes in this case, reducing a_p to meet the requirements. Furthermore, in the case of contours, since a_e was very limited (as mentioned above), it was sometimes necessary to perform multiple passes in the radial direction as well. This ensured compliance with the recommended catalog values, avoiding tool wear issues (e.g., the contour operation on the curved surface: CS_C). Finally, for the spindle rotational speed requirement, the formula remained the same as in the face milling case:

$$n = \frac{1000 \cdot v_c}{DC \cdot \pi}$$

Table 9: Peripheral Category

Code_op.	**ae**	**ap**	**Vc**	**fz**	**n [rpm]**	**Pc [W]**
SG_C	3	17	175	0.09	2785.21	10467.10
SCE_C	5	12.8333	235	0.12	3740.14	14892.57
CS_C	12.5	14	175	0.115	2228.17	13335.46

For the missing units of measurement in the table, please refer to the notations in the first paragraph.

Drilling case study

Drilling covers methods of making round holes in a workpiece with a metal cutting tool called drill bit. Through our manufacturing process, we perform various types of drilling to create holes A, B, C, and D, which can be classified into four distinct methods:

- **Drilling**: as roughing operation in through holes.
- **Pilot Drilling**: to realize the guided hole for the next thread.
- **Chamfer Drilling**: to realize countersink holes.
- **Step Drilling**: to realize a counterbore from existing hole.

We illustrate in the next section the applied procedure for drilling as general operation, thus, to detail later the remaining three drilling methods, in case the decision-making process differs from the general case.

Drilling 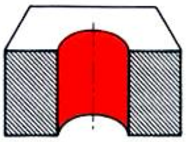 *Holes A and D*

The choice of drill depends on these basic parameters: **workpiece material**, **diameter**, **depth**, and **quality** (tolerance, surface finish).
First, the type of hole (in terms of diameter and depth) must be considered when selecting the cutting diameter and the maximum hole depth, as they appear in the catalog as **DC** and **LU**. The plot below links the hole type with the recommended drill tool category, dividing the choice into three main tool types:

- **Indexable insert drills**
  - medium and large diameter
  - medium tolerance
  - blind holes requiring a flat bottom
  - boring operations
- **Solid carbide drills**
  - small diameter
  - precision tolerance hole
  - large range of depth of cut
- **Exchangeable tip drils**
  - medium diameter
  - close hole tolerances
  - short to relatively deep holes

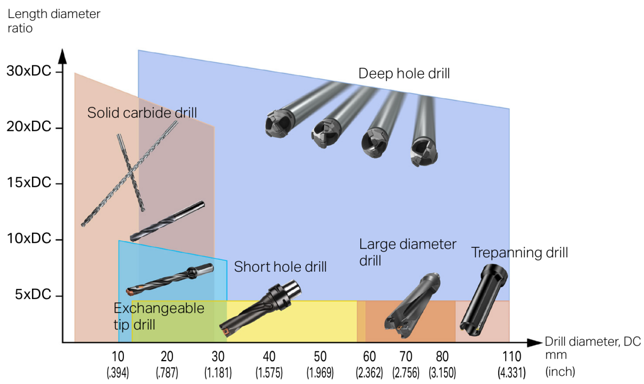

After having chosen the most suitable drill category (e.g. solid carbide for hole A and an indexable insert drill for hole D), we browse through the catalog in search of a tool that meets the following requirement:

$$\boldsymbol{ULDR} \geq \frac{\boldsymbol{LU}}{\boldsymbol{DC}}$$

Noting that since different ULDR sizes are listed in the catalog, we are looking for the smaller one that fits our requirements, to minimize bending moments and so tool deflec-

tion.
Therefor, the validation of the selected tool involves the verification of the hole tolerance by looking to the **TCHA** - achievable hole tolerance - parameter, which has to be less than or equal to the recommended hole tolerance, which is **H10** for both the through holes A and D that we are considering. The solid carbide tools have all a TCHA equals at least to H9, so that the tolerance is always satisfied. Regarding the tighter tolerance requirements **H7** for holes D and B, we match them with reaming for holes B and boring for hole D (boring has to be selected due to the large diameter of hole D).

Another important requirement includes the coolant method: we are looking for an **internal coolant supply**, which is always the first choice in executing deep holes ($ULDR > 3 \times DC$) as holes A and D, to improve chip formation and chip evacuation.

The next step, after tool choice, is the selection of its **grade** and of the **cutting data**; this last one will be used, together with other tool parameters (e.g. tip angle) to determine cutting power and spindle angular velocity, to finally verify the feasibility of the operation, given our spindle power and speed limitations. For both solid carbide drills and drill tips in exchangeable tip drills, there are tools specifically optimized for our material, which we consider as the first choice. Alternatively, multi-material drills are available, utilizing the same grade across various material groups.

The workpiece material, together with grade, influences also the cutting data selection, which are listed in the catalog as ranged values depending on the MC code classification. The cutting speed $\mathbf{V_c}$ can be determined either within a recommended range, $[V_{\text{cmin}}, V_{\text{cmax}}]$, where we use the arithmetic mean between min and max values as V_{start} value; or from a specified range format, $[V_{\text{cmin}} : V_{\text{start}} : V_{\text{cmax}}]$, in which case the provided V_{start} value is directly used.
Similarly, the feed per tooth $\mathbf{f}_\text{z}$ depends on both the material and the **DC** range, as specified in the catalog using the same range format as the cutting speed. For $\mathbf{f}_\text{z}$, we follow the same approach, using the reported $\mathbf{f}_\text{start}$ as the starting value.

Remarks on cutting data:

- Sometimes in the catalog, they are listed as associated with our MC code but for different hardness values. In such cases, we derive $f_\text{z}]$ and $V_\text{c}]$ through linear interpolation.

- For some tools, such as the CoroDrill 861 for deep holes, the recommended values are referred only for unalloyed steels of the groups P.1.1 and P.1.2, which are both more ductile than our material, due to the low carbon presence. Hence, we approximate our material as P.1.2, noting that for similar unalloyed steels V_c and f_z values in the catalog are almost the same, and that our material would be indeed more affected by chip breaking (deteriorating surface finishing) and abrasive flank wear (decreasing tool life). Then, by considering the properties of our material with respect P.1.2, and considering that during cutting power verification we normally aim to select V_max and f_max to minimize the cutting time t_c, we have decided in this case to try maximize f_z rather than V_c, because an higher V_c would increase the already high tendency of our material in having a flank wear (noting also that a too low

V_c increases bue behavior which is actually a relevant issue only in more ductile materials), while an higher f_z is indeed desiderable to make chip breaking more difficult.

At this point we can collect all the remaining tool parameters, to compute the **cutting power $\mathbf{P_c}$** and the **spindle rotational speed n**, in order to verify the feasibility of the operation given our machine tool limitations $\mathbf{P}_{max}$ and $\mathbf{n}_{max}$. To calculate the cutting power, we use the formula shown below, which applies to solid carbide drills, as well as to exchangeable and indexable ones.

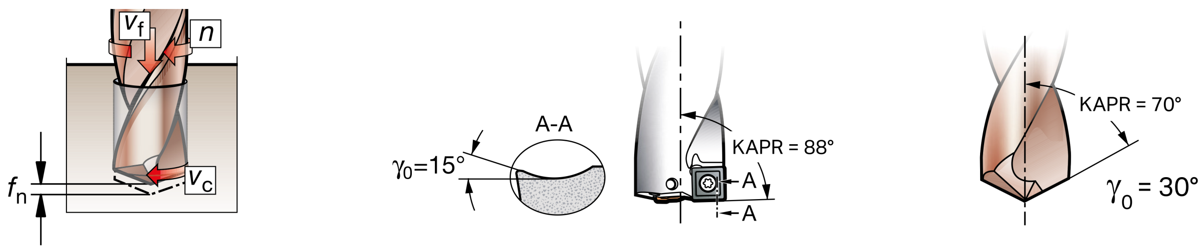

$$P_c = \frac{f_n \times v_c \times \mathrm{DC} \times k_c}{240 \times 10^3}\,\mathrm{kW} \qquad k_c = (k_{c1} \times (f_z \times \sin \mathrm{KAPR})^{m_c}) \times \left(1 - \frac{\gamma_0}{100}\right)$$

$$n = \frac{1000 \times V_c}{D \times \pi}$$

We can therefore obtain the tool's final parameters from the catalog: tip angle SIG and so $KAPR = \frac{SIG}{2}$, orthogonal rake angle γ_0, and the number of cutting edges z, which is always equal to 2 in twist drills.
We can now iterate the power and speed validation procedure, starting with the initial values $\mathbf{f}_{start}$ and $\mathbf{V}_{start}$. Both parameters are incrementally increased until either feasibility is violated or the upper limits, $\mathbf{f}_{max}$ and $\mathbf{V}_{max}$, are reached.

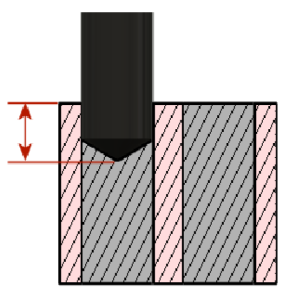

Peck Depth

Since we are drilling deep holes ($ULDR > 3 \times DC$), we configure in *Fusion* a **deep drilling - full retract cycle**, where the drill penetrates the material incrementally, advancing by a specified depth (called a "peck") during each drilling step. After each peck, the drill retracts completely out of the hole, allowing chips to be evacuated and reducing heat accumulation. This is especially important for deep holes, where chips can accumulate and lead to tool wear or breakage.

Considerations regarding drilling in hole D

Hole D has a medium diameter and a low ULDR ratio, a type of hole that needs a short hole drill, namely an **indexable insert drill**, which is a single cutting edge drill, with a central and a peripheral insert. The hole D will require boring as finishing operation to satisfy the H7 geometrical requirement, and since boring works with at most a depth of cut of $a_{\text{pmax}} = 0.5mm$, we have to use a drill with at least $DC = 51mm$.

The tool selection process also includes choosing the central and peripheral inserts, guided by the size recommendations provided in the catalog adjacent to our tool. Given the low power requirements, we opted for high-feed machining, selecting the GR geometry for our inserts. The grade of the inserts was chosen following the recommendations based on ISO material group.

For cutting data selection, the feed velocity is determined by the diameter range and the geometry of the insert, while the cutting speed range depends on the grade of the peripheral inserts.

Pilot Drilling

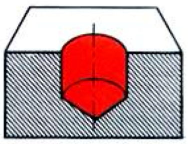

Holes B and C

Threads require the creation of a pilot hole, whose diameter (obviously smaller than the nominal diameter of the thread) is calculated using the following formulas, which hold for both threads performed with tapping and thread milling:

$$D = TD - TP \qquad \begin{aligned} D &: \text{hole diameter} \\ TD &: \text{nominal thread diameter} \\ TP &: \text{thread pitch} \end{aligned}$$

Step Drilling

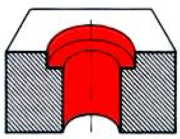

Holes B

We perform step drilling to create counterbores above holes B, leaving a 0.2 mm stock that will be removed later during the reaming operation. For both counterbore and countersink holes, the optimal approach is to combine the operations in a single step with the pilot hole using a **step and chamfer drill**. This type of drill has two tips with different diameters, which allows for a reduction in machining time and improves the concentricity of the counterbore/countersink relative to the future threaded hole. Unfortunately, we were unable to find a step drill that matches our required dimensions. This is because such tools are more common for softer materials, where they are less prone to wear. Consequently, we must execute first the pilot hole and the the counterbore using still a general drilling tool, but with a tip angle $SIG = 180$, which can be found in mitsubishi catalog.

For the verification of power and angular velocity, **step drilling** can be associated with a **reaming** operation, as both involve removing stock to enlarge an already existing hole. The formulas provided below therefore apply to both step drilling and reaming (noting that the number of cutting edges in reaming will be greater).

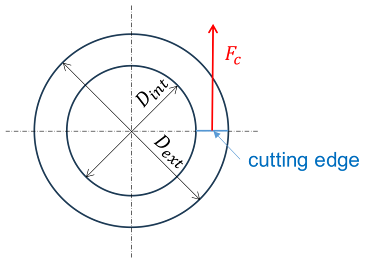

$$A_d = \frac{f_z}{2} \cdot (DC_{\text{ext}} - DC_{\text{int}})$$

$$F_c = k_c A_d$$

$$T_c = Z \frac{F_c \cdot (DC_{\text{ext}} - DC_{\text{int}})}{4}$$

$$P_c = T_c \frac{2\pi n}{60}$$

Chamfer Drilling

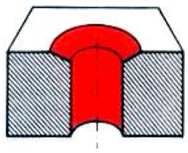

Holes C

In general, a countersink at the top of an hole is a good machining practice, when executing threads, for the following reasons:

- to avoid creating a raised **bur**, namely a portion of sharp material at machining edge, which can prevent a mating part (e.g a bolt) to properly seating with a coupled flat surface;
- when the mating is placed on the potential bur, it forces down and effectively deforming the internal thread and so risking a cross thread;
- it improves the starting of the threading machining operation;

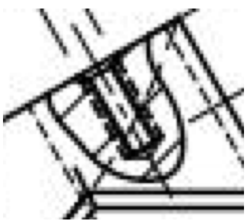

Countersink

Looking at the holes C in 2D draw, we don't see any specified geometrical requirement in terms of countersink size and angle, in fact it doesn't exist a specific DIN/ISO standard for chamfers; sometimes the external diameter and depth are specified with draws but in our case it has been given us the freedom of choice.

Chamfer angles are of 90°–120°: we choose 90° as the most common one.

A good and common practice is to apply a chamfer diameter of additional length in the range $0.0010'' - 0.0015''$ ($0.254\,\text{mm} - 0.381\,\text{mm}$) with respect to the thread nominal diameter TD: considering holes C we select the maximum approximated tolerance $D_{\text{chamfer}} = 7.40\,\text{mm}$.

Just like in the case of counterbore machining, there is no catalog tool that matches our conditions for chamfer drilling. In fact, there would be a tool with $DC_2 = D_{\text{chamfer}}$ and a tip angle of 90 degrees, but with a different LU from the hole depth (including tip length, as it is a blind hole). For this reason we have decided to machine the countersink using a general drill with $SIG = 90°$, which can be easily found in Mitsubishi catalog, among the **solid carbide drills for centering and chamfering**.

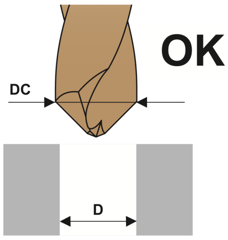

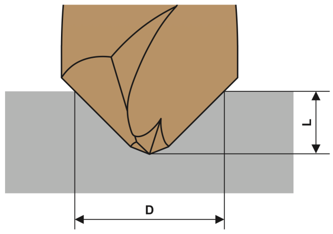

Choice of DC when chamfering

The Mitsubishi Material catalog recommends that with respect to guide hole diameter $\boldsymbol{D}$, the selection of drill diameter must be in the range:

$$D < DC < 2D$$

Considering holes C the inequality is verified ($6mm < 10mm < 12mm$).

Table 10: Drlling Operations

Code_op.	DC	depth	kc	fz	Vc	Pc [w]	n [rpm]
HA_D	8.00	111.67	2232	0.130	118	2280	4695
HB_D	6.75	50.00	2382	0.140	235	4400	11081
HC_D	6.00	12.00	2302	0.140	235	3780	12467
HC_CS	10.00	1.00	4156	0.044	75	11490	2377
HD_D	51.00	100.46	2375	0.240	240	7155	1469

Reaming case study

We perform reaming in Holes B to achieve the required tolerance grade H7 for counterbores.

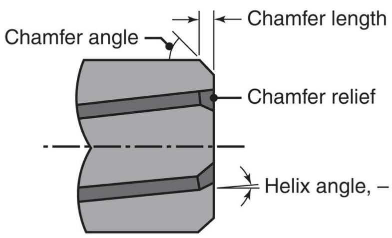

Remark: Reamers are not designed to achieve 90° angles at the bottom surface extremities, as would be the case with counterbore geometry. This is due to their chamfer angle, which results in a non-straight chamfer length. However, this is not a problem, as the bottom flat surface has already been defined during the drilling process. Reamers are intended for finishing, and their chamfer angle is necessary for chip evacuation and uniform load distribution. Without this, we could have used a flat end mill with a finishing pass.

The cutting power calculation in reaming follows the same procedure illustrated in the step drilling section.

Table 11: Reaming and Counterboring Operations

Code_op.	Dext	Dint	depth	kc	fz	Vc	Pc [w]	n [rpm]
HB_CB	9.8	6.75	5	3112	0.10	75	998	2426
HB_R	10	9.8	5	2914	0.13	180	1350	5730

Thread Milling case study

Regarding the threading operations of holes C and B, the thread can be machined either with **Tapping** or with **Thread Milling**. The following issues have led us to choose thread milling:

- Through holes B have a significant thread depth of 50mm. Since tapping must be performed in a single pass (to avoid asymmetries between consecutive passes that would compromise accuracy), and considering that both spiral point taps and straight flute taps (recommended tools for through holes) have an ULDR limited to $3 \times D$, we are compelled to choose thread milling in case of holes B.

- Thread milling, even if slower and much expensive than tapping, offers higher accuracy and better geometric tolerance.

- Tapping in blind holes can make chip evacuation more difficult, especially when machining materials that produce long chips, and there is an increased risk of tool breakage.

- Economic costs and machining time can be secondary considerations for ensuring technical feasibility, which is the primary objective of this manufacturing project.

For all these reasons, we perform holes B and C threads with a thread miller, resulting in a more uniform and simpler procedure.

The **thread miller** selection procedure starts with choosing between **indexable milling cutters** and **solid carbide milling cutters**. The second is the easiest choice, since this type of solid tools have a direct association with standard ISO M for threads, by means of **FTDZ** parameter.

CoroMill Pura
solid carbide

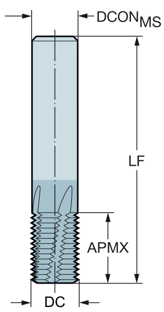

Among the solid carbide we can choose between **CoroMill Pura Solid** and **CoroMill 326**; since we need to perform multiple passes exploiting the maximum depth of cut we choose tools among CoroMill Pura tools, due to their higher **APMX**. We also consider CoroMill Pura tools with cylindrical shank, as shown in the image above, in order to ensure a shank diameter **DCON** always minor than the pilot hole diameter, to allow the tool to go down with multiple passes.

We select the tool by looking for $FTDZ = M8\times1.25$ for holes B and $FTDZ = M7\times1$ for holes C. Coromant Catalog doesn't have tools designed specifically for threaded holes with a even TD, but since it recommends to use a **DC** much smaller than **TD**, to limit $\boldsymbol{a_{e|\text{eff}}}$ and so preventing cross threading, we can exploit a thread mill with $FTDZ = M6 \times 1$ for holes C, noting that regarding this tool:

- $PT = 1mm \rightarrow$ in according with the required thread pitch
- $DC = 4.5mm < 0.7 \times TD = 4.9mm \rightarrow$ in according with the rule of thumb of keeping $DC < 70\% \times TD$

Thread milling produces threads with the circular ramping movement of a rotating tool. The lateral movement of the tool in one revolution creates the thread pitch, while 3 axis CNC interpolation is required to achieve the helical toolpath.

After confirming that $\boldsymbol{LF > d}$ and gathering all the operation parameters, including **z** (peripheral effective cutting edge), **TP**, **DC**, **APMX** and **TD**, we can proceed to select the recommended cutting data. The feed per tooth $\boldsymbol{f_z}$ and cutting speed $\boldsymbol{V_c}$, are chosen as approximate values corresponding to the nearest M10 thread listed in the catalog

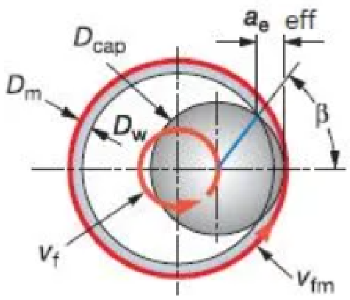

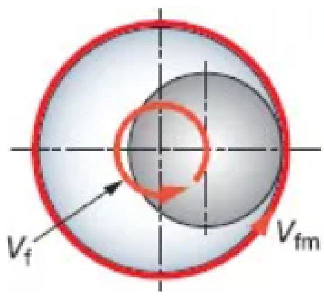

Cutting speed

$$V_c = \frac{DC \times \pi \times n}{1000}$$

Peripheral feed

$$V_{\text{fm}} = f_z \times z \times n$$

Radial Depth of Cut

$$a_e\text{eff} = \frac{D_m^2 - D_w^2}{4(D_m - DC)}$$

Remark: The feed per tooth provided in the catalog refers to the tangential feed along the thread diameter, corresponding to the peripheral feed velocity. It is unrelated to the penetration rate typical of operations like drilling; instead, it is directly linked to the chip thickness h_{ex}. However, many machines require a tool center feed (vf). In internal thread milling applications, the tool path of the periphery is faster than the movement of the tool center line. Feed rate programming on most milling machines is based on the center line of the spindle, and this must be included in thread milling calculations to maximize tool life and avoid vibration/tool breakdown.

Regarding the calculation of cutting power and the subsequent verification of the operation's compatibility with the machine's parameters, we can be confident that the operation is feasible for the following reasons:

1. By comparing each pass of the toolpath to an overlap of n face milling operations, with a cutting depth equal to the thread pitch, we can quickly observe that, while the cutting speeds V_c in thread milling are similar to those in drilling, the feed per tooth f_z is approximately 10 orders of magnitude smaller. Given that all face milling operations are deemed admissible, we can infer the feasibility of the operation by analogy.
2. After calculating the effective radial depth of cut $a_e$eff for both operations, and noting that it does not exceed 2 mm, we realize that the material removal rate (MRR) for this operation is significantly lower than that of the face milling operations conducted earlier.

To provide an approximate estimate of the cutting power, we can, by similarity, consider the formula used to calculate the power in a **Tapping** operation:

Cutting torque

$$T_c = \frac{TP^2 \times TD \times k_c}{8000}$$

Cutting power

$$P_c = \frac{T_c \times 2 \times \pi \times n}{60}$$

The cutting power calculation for threading operations on holes B and C, based on this formula, yields results in the range of 5 kW. This indicates that the estimate is even quite conservative, as explained in the previous two points.

Table 12: Thread Milling Operations

Code_op.	TD	TD	DC	depth	fz	Vc	Pc [w]	n [rpm]
HB_T	8	1.25	6	50	0.0290	124	5428	6578
HC_T	7	1.00	4.5	12	0.0235	132.5	4563	9372

Boring case study

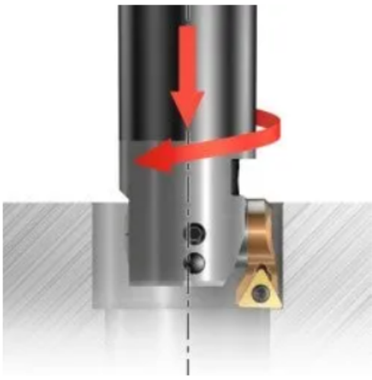

Boring is a machining process for enlarging or improving the quality of an existing hole. It is classified as a turning operation, therefore, boring does not use a drill tip, but rather a single-point cutting tool, which cut with one insert. We perform boring in hole D, to remove the $0.5mm$ radial stock left by the previous roughing drilling operation, to ensure the geometric tolerance requirement H7.

In order to satisfy our long overhang requirement of the *hole D* depth, we have selected the damped version of **CoroBore 825**, which ensures a hole tolerance of IT6, a cutting diameter range that contains our desired $DC = 52$ mm, and a functional length $LU > d = 100.46$ mm capable of easily reaching the entire hole depth (selecting the damped geometry with the smallest feasible LU, to minimize shank deflection).

In boring tools, the cutting diameter is provided as a range of values $[\boldsymbol{DCN}; \boldsymbol{DCX}]$, rather than a single value. This range accommodates the regulation of the tool's axial, radial, and angular extensions through the use of interchangeable modules that can be mounted with mechanical precision. These modules include the **boring cartridge** and **slide extensions**.
This approach allows for the selection of a tool by choosing the range that contains the desired cutting diameter, $DC = 52mm$. The exact diameter is then achieved by coupling the inserts via the cartridge and slide extensions, enabling precise adjustment of the radial offset.

The computation of cutting power and angular spindle speed in boring follows these formulas:

Cutting speed

$$n = \frac{V_c \times 1000}{DC \times \pi}$$

Cutting power

$$P_c = \frac{f_z \times a_p \times k_c \times V_c}{60 \times 1000} \times (1 - \frac{a_p}{DC})$$

When selecting the cutting data, we considered that the maximum feed rate in fine boring is constrained by the desired surface finish. In our case, this is dictated by the geometric tolerance H7, which typically corresponds to a surface roughness of $R_a \in [0.8, 1.6]\ \mu m$. To remain conservative, we opted for a feed rate f that achieves $R_a = 0.8\ \mu m$.

Table 13: Boring Operation

Code_op.	DC	ap	depth	kc	fz	Vc	Pc [w]	n [rpm]
HD_B	51	0.50	100.46	3111	0.10	900	2310	5509

5 Discussion on Technical Requirements

In this final section, we present the technical requirements (2D drawing below) and discuss how we are able to meet them by dividing the considerations into three categories:

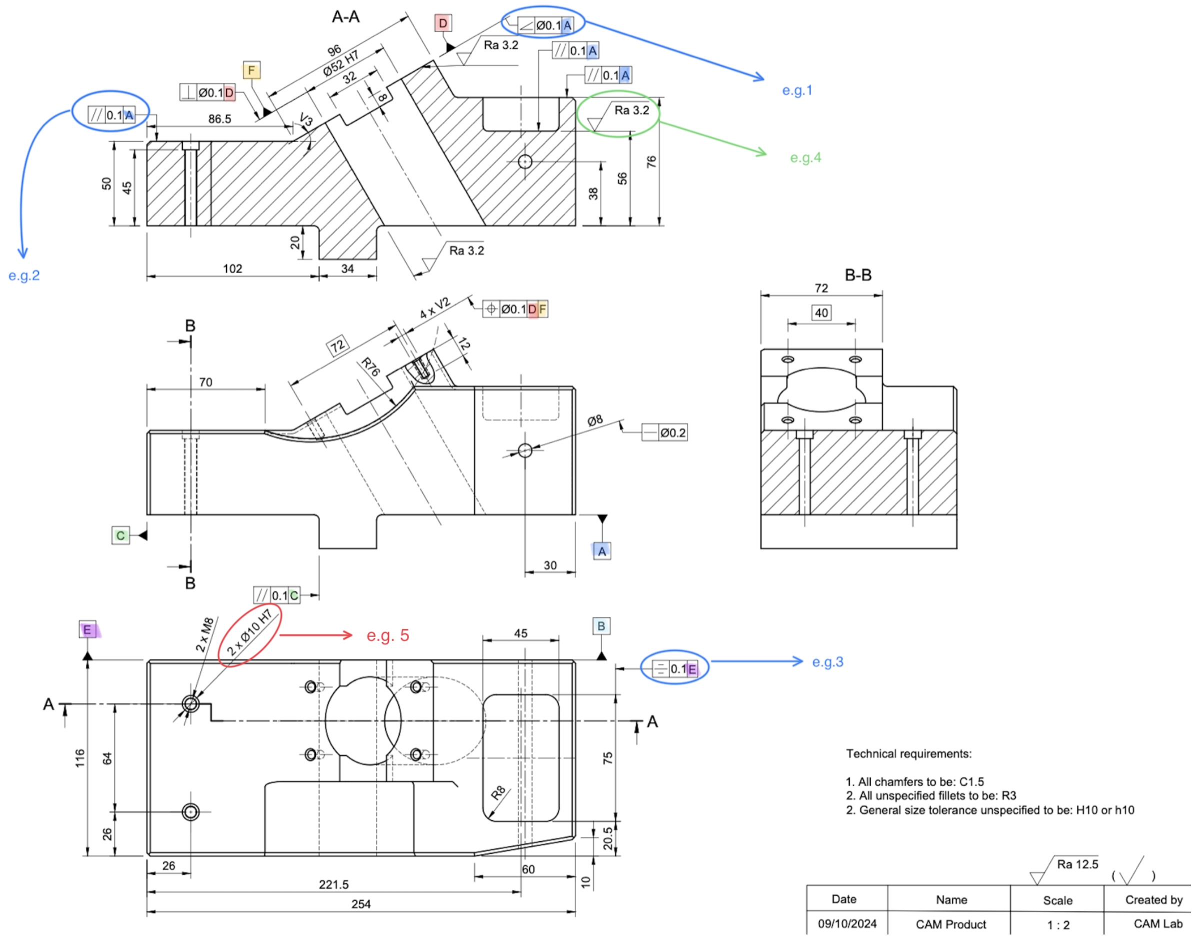

- **Geometric tolerances**: Regarding geometric tolerances, including requirements for parallelism, perpendicularity, etc., it was not necessary to input specific parameters into Fusion 360. Instead, it was primarily a matter of selecting the correct part positioning and, consequently, choosing the set ups in an order that allowed us to meet these geometric requirements (as illustrated in Section 3.2).
For example, to ensure parallelism relative to a datum, we designed the setups to be sure to machine the part parallel to that datum. In cases where flipping the part was necessary, we ensured it could be rotated 180 degrees to align again perfectly with the datum, avoiding any uncertainty.
We applied the same approach for perpendicularity or other angular requirements relative to a datum. Occasionally, we also selected an appropriate sequence of operations, such as for **Special Requirement 1** described in Section 2.3.

- **Dimensional tolerances**: We successfully met the closer H7 size tolerance for the stepped hole B and the large through hole D by applying the previously described reaming and boring operations, respectively (details in section 4). Both processes are designed as surface finishing operations to refine and enlarge existing holes. To ensure compliance with the H7 tolerance, we referred to the **TCHA** parameter of the boring tools in the catalog, verifying that it satisfied an IT grade of H7 or better. For reaming tools, we already knew that most were capable of achieving an IT6 grade

- **Roughness requirements**:

  1. **Face Milling with Inserts**: Having the nose radius (r) available in the catalog, it was sufficient to apply the formula studied during theory lessons to calculate the roughness:

  $$R_a = \frac{f_z^2 \cdot 1000}{32 \cdot r}$$

  We verified that this value was less than or equal to the required roughness for the corresponding surface.

  Table 14: Face Milling Operations - RA and Nose Radius

Code_op.	RA [μm]	**Nose Radius [mm]**
BS_F	1.633	1.5
SD_F	1.633	1.5
TS_F	1.633	1.5
SA_F	1.633	1.5
SB_F	1.519	1.5

  2. **Slab Milling (e.g. Contours)**: Similarly, to verify roughness requirements, it was sufficient to know the tool radius (R) and the feed per tooth (f_z), and calculate roughness using the formula:

  $$R_a = \frac{f_z^2 \cdot 1000}{32 \cdot R}$$

  Table 15: Peripheral Category - Roughness

Code_op.	**RA** [μm]
SG_C	0.02531
SCE_C	0.04500
CS_C	0.03306

  3. **Face Milling with Flat End Mills (Roughing and Finishing)**: This case was less straightforward. Since neither the nose radius nor the secondary entering angle (k'_r) was available (and k'_r appeared to be 0 in the catalog), we faced some challenges. To address this issue, we adopted a reverse approach without explicitly calculating the roughness.

  Although k'_r is considered 0 in the catalog, we know that in practice, perfect perpendicularity in a tool is unlikely. A k'_r of 0 would imply zero roughness, resulting in a perfectly smooth surface, which is an ideal but unrealistic scenario. In reality, k'_r will be close to but not exactly 0.(N.B: Given such a small value for k'_r , it is crucial to consider potential friction issues, even though the software does not impose any explicit limitations in this regard).

Therefore, our solution was to start from the target roughness for the surface and, using the inverse formula of $R_a = \frac{f_z}{4 \cdot (\cot k_r' + \cot k_r)} \cdot 10^3$ (assuming $k_r = 90°$, so $\cot(90°) = 0$), calculate the maximum k_r' required to meet the roughness specification:

$$k'_{r,\max} = \arctan\left(\frac{4 \cdot R_{a,\text{target}}}{f_z \cdot 1000}\right)$$

Based on this calculation, we consistently obtained values greater than 10° (approximately 14° in the most stringent finishing case). We are confident that the roughness requirements are always met because the k_r' of flat end mills is undoubtedly below the calculated limits, which are large enough to be noticeable to the naked eye .

Table 16: Face with Flat end Mill - RA and Kr' Values

Code_op.	$RA(Radial)$ [μ**m**]	$Kr'(Axial)$ [**deg**]
BS_P		29.055
TS_P_D		23.499
TS_P_U		23.499
SF_P		23.499
SH_P		23.499
PO_P	0.025	32.005
CS_T	0.009	
PO_P_F		14.359
SF_P_F		14.359
SL_P	0.016	45.000

To conclude this section, we present some final observations. In particular, for operations such as pocketing or other processes where the tool comes into contact with both radial and axial surfaces of the workpiece (Figure 7, Slot), we calculated two roughness values: one for each surface.

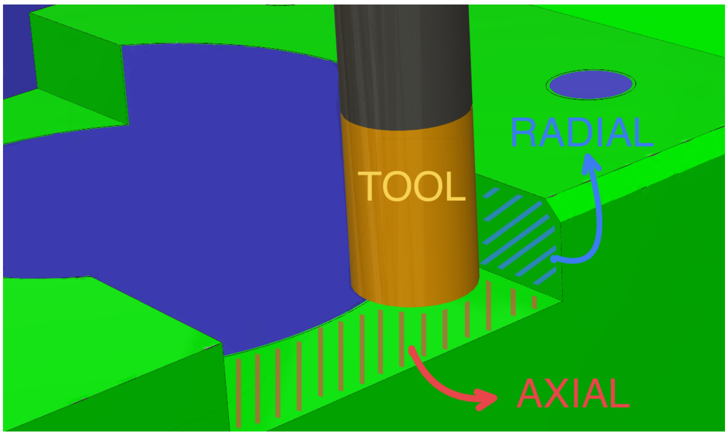

Figure 2: Slot

This was interpreted as performing pocket milling.

Additionally, in cases of high roughness requirements (finishing operations), we consistently left a small portion of stock material and conducted a separate finishing operation, even when it was not strictly necessary to meet the requirements. We chose to do this to align with the practices taught during lab sessions throughout the semester and because it is considered good practice.

4. **Chamfer and Fillet**: standard roughness formulas mentioned in section 1.

Table 17: Chamfer and Fillet - RA and Nose Radius

Code_op.	RA [μ**m**]	**Nose Radius [mm]**
FI_B	0.017	3
FI_A	0.017	3
PO_FI	0.017	3
CH_1	4.049	
CH_2	4.049	
CH_3	4.049	